Contribution from the Department of Chemistry,
University of Toronto, Toronto, Ontario, Canada M5S 1A1

Binuclear Phosphido-Bridged CrPt, MoPt, and WPt Complexes. Synthesis of $(CO)_4M(\mu\text{-}PPh_2)_2Pt(PR_3)$ Complexes and Effect of the M→Pt Donor Bond on the Reactivity of the Carbonyl Ligands

John Powell,* Christian Couture, Michael R. Gregg, and Jeffery F. Sawyer

Received November 2, 1988

The series of complexes $(OC)_4M(\mu\text{-}PPh_2)_2Pt(PR_3)$ (**1**; M = Cr, Mo, W; PR_3 = PCy_3, PPh_3, PEt_3) have been prepared from the reaction of PPh_2H with $(OC)_4M(\mu\text{-}H)(\mu\text{-}PPh_2)PtL_2$ (L_2 = $(PPh_3)_2$, $(CO)(PCy_3)$) and from the reaction of $(OC)_4M(PPh_2Li)_2$ with *cis*-$PtCl_2(PEt_3)_2$. The molecular structure of $(OC)_4Mo(\mu\text{-}PPh_2)_2Pt(PEt_3)$ was determined by single-crystal X-ray diffraction. (Crystal data: $C_{34}H_{35}MoO_4P_3Pt$ crystallizes in space group *Pbca* with $a = 18.381$ (3) Å, $b = 16.989$ (2) Å, $c = 22.462$ (5) Å, $V = 7014$ Å^3, and $D_{calc} = 1.69$ g cm^{-3} for $Z = 8$; R (R_w) = 0.0363 (0.0440) for 3225 data with $I \geq 3\sigma(I)$.) The Mo atom has pseudooctahedral geometry and is linked by two bridging PPh_2 ligands to a pseudo-trigonal-planar platinum center. The Mo–Pt distance is 2.766 (1) Å, indicative of a Mo→Pt dative bond. Addition of PhLi to $(CO)_4M(\mu\text{-}PPh_2)_2Pt(PCy_3)$ gives the benzoylate $(OC)_3(PhCOLi)M(\mu\text{-}PPh_2)_2Pt(PCy_3)$, which reacts with CH_3SO_3F to give the carbene complexes $(OC)_3\{PhC(OMe)\}M(\mu\text{-}PPh_2)_2Pt(PCy_3)$. Reaction of PhLi with $(OC)_4M(\mu\text{-}PPh_2)_2Pt(PR_3)$ (PR_3 = PPh_3, PEt_3) gave mixtures of $(OC)_3(PhCOLi)M(\mu\text{-}PPh_2)_2Pt(PR_3)$ and $[(OC)_4M(\mu\text{-}PPh_2)_2Pt(Ph)(PR_3)]Li$. The increased reactivity of $(OC)_4M(\mu\text{-}PPh_2)_2Pt(PR_3)$ toward nucleophilic addition at CO vis à vis *cis*-$M(CO)_4(PR_3)_2$ complexes (unreactive toward RLi) and the unusual stereochemistry (PhCOLi trans to P_μ in $(OC)_3(PhCOLi)M(\mu\text{-}PPh_2)_2Pt(PR_3)$) are ascribed to electronic effects associated with the presence of a M→Pt metal–metal bond. Extended Hückel MO calculations indicate that nucleophilic attack at a CO trans to P_μ can be considered to be frontier orbital and charge controlled.

Introduction

In recent years a range of diorganophosphido-bridged, early- to late-transition-metal heterobimetallic compounds have been synthesized and studied.[1–17] Interest in such compounds has focused on the stabilization of ligands in unusual coordination modes, ligand reactivities in bimetallic systems, and the stability/reactivity of bimetallic formyl, acyl, carbene, and related systems involved in carbon monoxide reduction chemistry. A general synthetic approach that has yielded a range of interesting bis(diphenylphosphido)-bridged heterobimetallics involves the deprotonation of metal-coordinated secondary phosphines followed by reaction of the resultant dianion with a transition-metal halide. Particularly relevant to this paper is the example shown (eq 1).[1,18] The metal–metal-bonded complexes of type **1** and analogues that

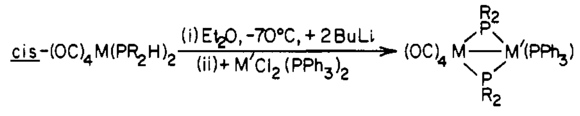
(1)

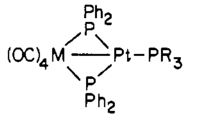

1	a	b	c	d	e	f	g	h	i
M =	Cr	Cr	Cr	Mo	Mo	Mo	W	W	W
R =	Ph	Et	Cy	Ph	Et	Cy	Ph	Et	Cy

have been prepared in this manner and structurally characterized by X-ray diffraction methods include $(OC)_4W(\mu\text{-}PPh_2)_2IrH(CO)(PPh_3)$,[13] $(OC)_4W(\mu\text{-}PPh_2)_2IrH(COD)$,[7] $(OC)_4W(\mu\text{-}PPh_2)_2Re(CO)_3Me$,[10] $(OC)_4W(\mu\text{-}PPh_2)_2Pt(PPh_3)$,[18] and $(OC)_4Mo(\mu\text{-}PCy_2)_2Pd(PPh_3)$.[1] The complexes $(OC)_4W(\mu\text{-}PPh_2)_2IrH(CO)(PPh_3)$ and $(OC)_4W(\mu\text{-}PPh_2)_2Re(CO)_3Me$ are reported to react with RLi to give the acylate/benzoylate derivatives $(OC)_3(RCOLi)W(\mu\text{-}PPh_2)_2IrH(CO)(PPh_3)$ and $(OC)_3(RCOLi)W(\mu\text{-}PPh_2)_2Re(CO)_3Me$, respectively.[10,13] However, the complexes *cis*-$M(CO)_4(PR_3)_2$ (M = Cr, Mo, W)[19] are unreactive toward RLi, and addition of RLi to $(OC)_4W(\mu\text{-}PPh_2)_2Zr(Cp)_2$[3]/$(OC)_4Mo(\mu\text{-}PEt_2)_2Hf(Cp)_2$[4] (no metal–metal bond) did not lead to isolable acylate/benzoylate products. In contrast the complexes $(OC)_4M(\mu\text{-}PPh_2)_2M(CO)_4$, which have a metal–metal bond, *are* reactive toward RLi addition;[20] this clearly points toward the activation of CO to nucleophilic addition in these dimeric complexes being influenced by the presence or absence of direct metal–metal bonding. Previous reports of the complexes $(OC)_4W(\mu\text{-}PPh_2)_2Pt(PPh_3)$[18] and $(OC)_4Mo(\mu\text{-}PCy_2)_2M'(PPh_3)$ (M = Ni, Pd, Pt)[1] did not comment on the possible reaction of these compounds with RLi reagents.

In this paper we describe several new synthetic routes to the

---

(1) Loeb, S. J.; Taylor, H. A.; Gelmini, L.; Stephan, D. W. *Inorg. Chem.* **1986**, *25*, 1977.
(2) Gelmini, L.; Stephan, D. W. *Inorg. Chem.* **1986**, *25*, 1222.
(3) Targos, T. S.; Rosen, R. P.; Whittle, R. R.; Geoffroy, G. L. *Inorg. Chem.* **1985**, *24*, 1375.
(4) Baker, R. T.; Tulip, T. H.; Wreford, S. S. *Inorg. Chem.* **1985**, *24*, 1379.
(5) Mercer, W. C.; Geoffroy, G. L.; Rheingold, A. L. *Organometallics* **1985**, *4*, 1418.
(6) Rosenberg, S.; Lockledge, S. P.; Geoffroy, G. L. *Organometallics* **1986**, *5*, 2517.
(7) Rosenberg, S.; Mahoney, W. S.; Hayes, J. M.; Geoffroy, G. L. *Organometallics* **1986**, *5*, 1065.
(8) Rosenberg, S.; Whittle, R. R.; Geoffroy, G. L. *J. Am. Chem. Soc.* **1984**, *106*, 5934.
(9) Mercer, W. C.; Whittle, R. R.; Burkhardt, E. W.; Geoffroy, G. L. *Organometallics* **1985**, *4*, 68.
(10) Powell, J.; Gregg, M. R.; Sawyer, J. F. *Inorg. Chem.* **1988**, *27*, 4526.
(11) Rosenberg, S.; Geoffroy, G. L.; Rheingold, A. L. *Organometallics* **1985**, *4*, 1184.
(12) Geoffroy, G. L.; Rosenberg, S.; Shulman, P. M.; Whittle, R. R. *J. Am. Chem. Soc.* **1984**, *106*, 1519.
(13) Breen, M. J.; Shulman, P. M.; Geoffroy, G. L.; Rheingold, A. L.; Fultz, W. C. *Organometallics* **1984**, *3*, 782.
(14) Roberts, D. A.; Steinmetz, G. R.; Breen, M. J.; Shulman, P. M.; Morrison, E. D.; Duttera, M. R.; DeBrosse, C. W.; Whittle, R. R.; Geoffroy, G. L. *Organometallics* **1983**, *2*, 846.
(15) Harley, A. D.; Guskey, G. J.; Geoffroy, G. L. *Organometallics* **1983**, *2*, 53.
(16) Burkhardt, E. W.; Mercer, W. C.; Geoffroy, G. L.; Rheingold, A. L.; Fultz, W. C. *J. Chem. Soc., Chem. Commun.* **1983**, 1251.
(17) Burkhardt, E. W.; Mercer, W. C.; Geoffroy, G. L. *Inorg. Chem.* **1984**, *23*, 1779.
(18) Morrison, E. D.; Harley, A. D.; Marcelli, M. A.; Geoffroy, G. L.; Rheingold, A. L.; Fultz, W. C. *Organometallics* **1984**, *3*, 1407.
(19) Darensbourg, D. J.; Darensbourg, M. Y. *Inorg. Chem.* **1970**, *9*, 1691.
(20) Shyu, S. G.; Wojcicki, A. *Organometallics* **1984**, *3*, 809.

0020-1669/89/1328-3437$01.50/0 © 1989 American Chemical Society

Table I. $^{31}P\{^1H\}$ NMR and Analytical Data for the Complexes $(OC)_4\overline{M(\mu\text{-}PPh_2)_2Pt}(PR_3)$ (**1a–i**)

	M	R	δP		$J_{^{31}P-^{31}P}$, Hz	$J_{^{195}Pt-^{31}P}$, Hz		$J_{^{183}W-^{31}P}$, Hz	anal. calcd (found)	
			μ-PPh$_2$[a]	PR$_3$[b]		μ-PPh$_2$	PR$_3$	μ-PPh$_2$	C	H
1a	Cr	Ph	226	52	62	2977	5196		55.72 (55.16)	3.53 (3.98)
1b	Cr	Et	234	43	61	2936	4917		48.11 (47.83)	4.13 (4.02)
1c	Cr	Cy	231	70	58	2970	4915		54.70 (54.60)	5.25 (5.57)
1d	Mo	Ph	202	49	58	2750	5256		53.35 (53.82)	3.38 (4.03)
1e	Mo	Et	195	30	58	2718	4938		45.78 (45.28)	3.96 (3.93)
1f	Mo	Cy	207	67	55	2764	4920		52.44 (52.13)	5.03 (5.40)
1g	W	Ph	173	47	47	2668	5113	145	*c*	*c*
1h	W	Et	176	33	48	2642	4919	154	41.74 (41.53)	3.58 (3.75)
1i	W	Cy	180	65	45	2687	4896	148	48.40 (48.87)	4.64 (4.96)

[a] 1:4:1 triplet of 1:1 doublets. [b] 1:4:1 triplet of 1:2:1 triplets. [c] See ref 18.

series of molecules $(OC)_4\overline{M(\mu\text{-}PPh_2)_2Pt}(PR_3)$ (**1a–i**; M = Cr, Mo, W; PR$_3$ = PEt$_3$, PPh$_3$, PCy$_3$) together with an X-ray diffraction study of $(OC)_4\overline{Mo(\mu\text{-}PPh_2)_2Pt}(PEt_3)$. Unlike the mononuclear analogues $M(CO)_4(PR_3)_2$,[19] the complexes **1** and structural analogues are susceptible to nucleophilic addition of RLi. The "source" of CO activation *and* the observed stereochemistry of the resultant acylate/benzoylate derivatives are ascribed to a consequence of the effect of direct M→Pt bonding. (Previous studies of $(OC)_4\overline{W(\mu\text{-}PPh_2)_2W}(CO)_4$/RLi systems suggested that steric effects controlled the stereochemistry of RLi addition.[20])

Results

Synthetic routes to the complexes $(OC)_4\overline{M(\mu\text{-}PPh_2)_2Pt}(PR_3)$ (**1**; M = Cr, Mo, W; R = Et, Ph, Cy) are given in eq 1–4. Besides

$$2(OC)_5M(PPh_2Li) + \underline{cis}\ PtCl_2(PEt_3)_2 \longrightarrow \underline{1}b,e,h + M(CO)_5(PEt_3) + \text{other products} \qquad (2)$$

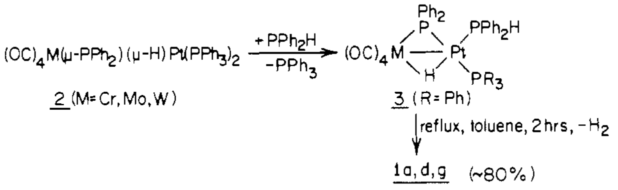

(3)

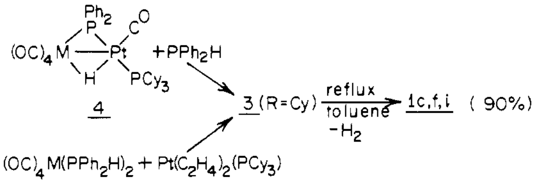

(4)

the previously established reactions of *cis*-$M(CO)_4(PPh_2Li)_2$ with *cis*-$PtCl_2(PR_3)_2$ (eq 1),[18] the complexes **1b,e,h** were also obtained from the reaction of $M(CO)_5(PPh_2Li)$ (M = Cr, Mo, W) with *cis*-$PtCl_2(PEt_3)_2$ in a 2:1 molar ratio (eq 2). Chromatographic workup of the reaction mixture gave **1b,e,h** (ca. 16% overall yield), $M(CO)_5(PEt_3)$, and other as yet undetermined products. Infrared monitoring of the reaction was consistent with the initial formation of $Pt(PEt_3)_2\{(\mu\text{-}PPh_2)M(CO)_5\}_2$ prior to rearrangement to the observed products. The most successful synthetic routes to **1** are those outlined in eq 3 and 4. Oxidative addition of $M(CO)_5(PPh_2H)$ to $Pt(C_2H_4)(PPh_3)_2$ gives $(OC)_4M(\mu\text{-}H)(\mu\text{-}PPh_2)Pt(PPh_3)_2$ (**2**) in high yield.[21] Reaction of **2** with 1 molar equiv of PPh$_2$H gives $(OC)_4M(\mu\text{-}H)(\mu\text{-}PPh_2)Pt(PPh_2H)(PPh_3)$ (<u>3; R = Ph</u>), which, on reflux in toluene for 2 h gives $(OC)_4\overline{M(\mu\text{-}PPh_2)_2Pt}(PPh_3)$ in ca. 80% yield. Oxidative addition of $M(CO)_5(PPh_2H)$ to $Pt(C_2H_4)_2(PCy_3)$ to give $(OC)_4M(\mu\text{-}H)(\mu\text{-}PPh_2)Pt(CO)(PCy_3)$ (**4**; R = Cy)[22] followed by the addition of PPh$_2$H and 2-h reflux (eq 4) provides $(OC)_4\overline{M(\mu\text{-}PPh_2)_2Pt}(PCy_3)$ complexes in ca. 90% overall yield. Complexes **1** and **3** are also obtained from the reaction of $M(CO)_4(PPh_2H)_2$ with $Pt(C_2H_4)_2(PCy_3)$ (eq 4). Spectroscopic and analytical data for the complexes **1** are given in Tables I and II. The structure and stereochemistry of the complexes **1** were determined by a single-crystal X-ray diffraction study of the complex $(OC)_4\overline{Mo(\mu\text{-}PPh_2)_2Pt}(PEt_3)$ (**1e**).[23]

Table II. Infrared Spectral Data

	M	R	ν(CO),[a] cm^{-1}
1a	Cr	Ph	2018 (s), 1940 (s, br), 1930 (vs, br)
1b	Cr	Et	2016 (s), 1938 (s, br), 1925 (vs, br)
1c	Cr	Cy	2015 (s), 1936 (s), 1923 (vs, br)
1d	Mo	Ph	2035 (s), 1952 (s, br), 1935 (vs, br)
1e	Mo	Et	2033 (s), 1954 (s, br), 1932 (s, br)
1f	Mo	Cy	2031 (s), 1948 (s, br), 1928 (vs)
1g	W	Ph	2032 (s), 1944 (s, br), 1927 (vs)
1h	W	Et	2031 (s), 1942 (s, br), 1923 (vs)
1i	W	Cy	2030 (s), 1941 (s, br), 1921 (vs)
8d	Mo	Ph	1978 (m), 1910 (m), 1875 (s)
8e	Mo	Et	1975 (m), 1900 (m), 1871 (s)
8f	Mo	Cy	1972 (m), 1905 (m), 1867 (s)
8g	W	Ph	1980 (m), 1908 (m), 1867 (s)
8h	W	Et	1970 (m), 1901 (m), 1862 (s)
8i	W	Cy	1969 (m), 1903 (m), 1860 (s)
9f	Mo	Cy	1991 (m, br), 1916 (vs, br)
9i	W	Cy	1995 (m, br), 1908 (vs, br)

[a] All in THF solutions. Abbreviations: s = strong, v = very, br = broad, m = medium.

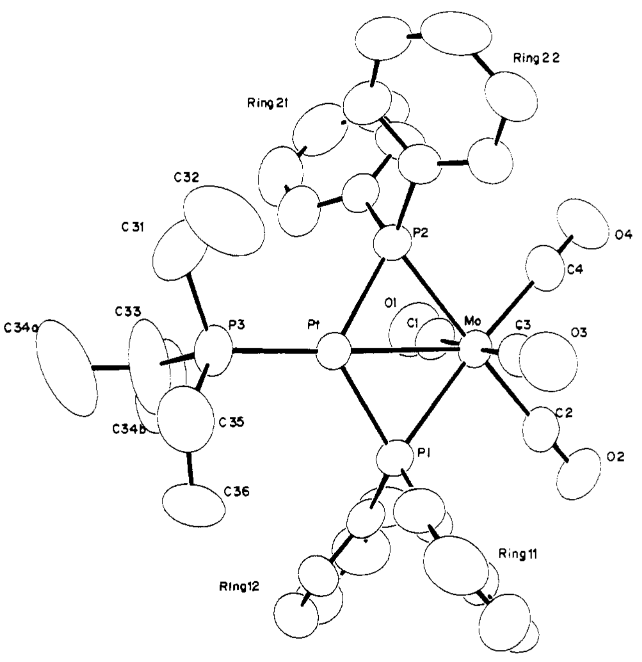

Figure 1. Molecular structure of $(OC)_4\overline{Mo(\mu\text{-}PPh_2)_2Pt}(PEt_3)$ (**1e**) as determined by single-crystal X-ray diffraction. Both disordered positions for atom C34 are indicated.

---

(21) Powell, J.; Gregg, M. R.; Sawyer, J. F. *J. Chem. Soc., Chem. Commun.* **1984**, 1149.

(22) Powell, J.; Gregg, M. R.; Sawyer, J. F. *Inorg. Chem.*, in press.

Table III. Positional Parameters and Their Estimated Standard Deviations for Complex **1e**[a]

atom	*x*	*y*	*z*	*B*, Å^2
Pt	0.09328 (2)	0.20638 (2)	0.01846 (2)	3.591 (6)
Mo	−0.00361 (4)	0.33095 (5)	0.01659 (4)	3.73 (2)
P1	0.0481 (1)	0.2523 (1)	−0.0681 (1)	3.80 (5)
P2	0.0542 (2)	0.2631 (2)	0.1033 (1)	3.87 (5)
P3	0.1723 (2)	0.1066 (2)	0.0218 (1)	5.02 (6)
O1	−0.1365 (4)	0.2181 (5)	0.0416 (4)	7.7 (2)
O2	−0.0787 (4)	0.4198 (4)	−0.0898 (3)	7.0 (2)
O3	0.1301 (4)	0.4459 (5)	−0.0012 (4)	7.3 (2)
O4	−0.0692 (5)	0.4417 (5)	0.1157 (4)	8.8 (2)
C1	−0.0885 (5)	0.2583 (6)	0.0303 (4)	5.1 (2)
C2	−0.0518 (5)	0.3865 (5)	−0.0512 (5)	4.7 (2)
C3	0.0836 (5)	0.4034 (5)	0.0063 (4)	4.4 (2)
C4	−0.0448 (6)	0.4030 (6)	0.0802 (5)	5.6 (3)
C31	0.2190 (8)	0.0975 (9)	0.0972 (6)	11.2 (4)
C32	0.2597 (9)	0.166 (1)	0.1117 (7)	13.4 (5)
C33	0.1302 (9)	0.0118 (7)	0.0142 (9)	12.3 (6)
C34A	0.185 (2)	−0.055 (2)	0.015 (2)	15 (1)[b]
C34B	0.063 (2)	−0.011 (2)	0.000 (2)	13 (1)[b]
C35	0.2494 (7)	0.1102 (8)	−0.0305 (6)	8.3 (4)
C36	0.2286 (9)	0.1049 (9)	−0.0945 (5)	10.4 (5)
C111	0.1051 (5)	0.3091 (5)	−0.1192 (4)	4.1 (2)
C112	0.1776 (6)	0.3209 (6)	−0.1062 (5)	5.3 (3)
C113	0.2202 (6)	0.3696 (7)	−0.1447 (5)	7.0 (3)
C114	0.1892 (7)	0.4049 (6)	−0.1890 (5)	7.6 (3)
C115	0.1169 (7)	0.3941 (6)	−0.2036 (5)	6.7 (3)
C116	0.0752 (6)	0.3472 (6)	−0.1677 (5)	5.1 (3)
C121	−0.0095 (5)	0.1947 (5)	−0.1178 (4)	4.4 (2)
C122	0.0227 (6)	0.1491 (6)	−0.1625 (5)	5.5 (3)
C123	−0.0190 (7)	0.1030 (7)	−0.1990 (5)	7.0 (3)
C124	−0.0926 (7)	0.1003 (6)	−0.1926 (5)	7.8 (3)
C125	−0.1238 (7)	0.1439 (8)	−0.1496 (6)	8.1 (4)
C126	−0.0832 (6)	0.1904 (7)	−0.1115 (5)	6.6 (3)
C211	−0.0068 (6)	0.2078 (6)	0.1520 (4)	4.7 (2)
C212	−0.0452 (7)	0.2439 (7)	0.1966 (5)	6.5 (3)
C213	−0.0936 (7)	0.2031 (8)	0.2318 (5)	7.8 (3)
C214	−0.1030 (7)	0.1261 (8)	0.2218 (6)	8.1 (4)
C215	−0.0669 (7)	0.0880 (7)	0.1798 (6)	7.7 (4)
C216	−0.0175 (6)	0.1298 (7)	0.1427 (5)	6.5 (3)
C221	0.1107 (5)	0.3169 (6)	0.1566 (4)	4.3 (2)
C222	0.1256 (6)	0.3963 (6)	0.1520 (5)	5.4 (3)
C223	0.1718 (7)	0.4336 (6)	0.1914 (5)	6.3 (3)
C224	0.2027 (6)	0.3905 (7)	0.2369 (5)	6.6 (3)
C225	0.1882 (7)	0.3113 (6)	0.2425 (5)	6.2 (3)
C226	0.1430 (6)	0.2750 (5)	0.2033 (5)	5.0 (3)

[a] All atoms were refined anisotropically, and their thermal parameters are given in the form of the isotropic equivalent thermal parameter defined as $^4/_3[a^2B_{11} + b^2B_{22} + c^2B_{33} + ab(\cos\gamma)B_{12} + ac(\cos\beta)B_{13} + bc(\cos\alpha)B_{23}]$. [b] Population parameter = 0.5.

Table IV. Selected Bond Distances (Å) and Bond Angles (deg)

Bond Distances

Pt–Mo	2.766 (1)	P1–C121	1.823 (10)
Pt–P1	2.254 (2)	P2–C211	1.829 (11)
Pt–P2	2.253 (3)	P2–C221	1.829 (10)
Pt–P3	2.234 (3)	P3–C31	1.904 (15)
Mo–P1	2.512 (3)	P3–C33	1.795 (14)
Mo–P2	2.500 (3)	P3–C35	1.843 (12)
Mo–C1	2.012 (11)	O1–C1	1.145 (11)
Mo–C2	1.999 (11)	O2–C2	1.146 (11)
Mo–C3	2.034 (10)	O3–C3	1.132 (11)
Mo–C4	2.029 (11)	O4–C4	1.126 (11)
P1–C111	1.829 (10)		

Bond Angles

Mo–Pt–P1	59.00 (7)	C1–Mo–C4	88.5 (4)
Mo–Pt–P2	58.69 (7)	C2–Mo–C3	88.7 (4)
Mo–Pt–P3	178.82 (9)	C2–Mo–C4	95.0 (4)
P1–Pt–P2	117.67 (9)	C3–Mo–C4	90.6 (4)
P1–Pt–P3	122.1 (1)	Pt–P1–Mo	70.72 (7)
P2–Pt–P3	120.2 (1)	Pt–P1–C111	120.8 (3)
Pt–Mo–P1	50.28 (6)	Pt–P1–C121	123.8 (3)
Pt–Mo–P2	50.34 (6)	Mo–P1–C111	114.3 (3)
Pt–Mo–C1	91.6 (3)	Mo–P1–C121	122.0 (4)
Pt–Mo–C2	131.2 (3)	C111–P1–C121	103.4 (5)
Pt–Mo–C3	87.5 (3)	Pt–P2–Mo	70.97 (7)
Pt–Mo–C4	133.7 (3)	Pt–P2–C211	118.8 (4)
P1–Mo–P2	100.60 (8)	Pt–P2–C221	125.9 (3)
P1–Mo–C1	94.8 (3)	Mo–P2–C211	116.3 (3)
P1–Mo–C2	80.9 (3)	Mo–P2–C221	121.4 (3)
P1–Mo–C3	86.4 (3)	C211–P2–C221	102.3 (5)
P1–Mo–C4	174.9 (3)	Pt–P3–C31	112.6 (5)
P2–Mo–C1	85.9 (3)	Pt–P3–C33	113.4 (6)
P2–Mo–C2	178.5 (3)	Pt–P3–C35	117.0 (5)
P2–Mo–C3	91.8 (3)	C31–P3–C33	101.9 (9)
P2–Mo–C4	83.6 (3)	C31–P3–C35	102.9 (8)
C1–Mo–C2	93.6 (4)	C33–P3–C35	107.5 (7)
C1–Mo–C3	177.6(4)		

Molecular Structure of $(OC)_4Mo(\mu\text{-}PPh_2)_2Pt(PEt_3)$ (1e). An ORTEP drawing of **1e** giving the atom-labeling scheme is shown in Figure 1. Final atomic positional parameters are given in Table III. Relevant bond angles and distances are given in Table IV. Neglecting the Mo–Pt interaction, the molybdenum exhibits an octahedral coordination geometry, while the platinum center has a trigonal-planar arrangement of the three phosphorus ligands. The acute Mo–P–Pt angles (71°) of the phosphido bridges are typical for metal–metal-bonded systems. The Mo–Pt bond distance of 2.766 (1) Å in **1e** is virtually the same length as that observed in $(OC)_4Mo(\mu\text{-}PCy_2)_2Pd(PPh_3)$[1] and $(OC)_4W(\mu\text{-}PPh_2)_2Pt(PPh_3)$[18] and is slightly shorter than the unsupported Mo–Pt bond length reported for *cis*-$(PPh_3)_2HPtMo(CO)_3Cp$ (2.839 (1) Å).[24a] Previously reported Mo–Pt bond lengths range from 2.65 to 2.91 Å.[24b]

Besides **1e**, other structurally characterized metal–metal-bonded systems containing the planar "$(\mu\text{-}P)_2PtL$" unit include $(OC)_4W(\mu\text{-}PPh_2)_2PtL$ (L = PPh_3 (**1g**), $MeO_2CC{\equiv}CCO_2Me$),[18] $(OC)_4Mo(\mu\text{-}PCy_2)_2Pd(PPh_3)$,[1] and $(PPh_3)Pt(\mu\text{-}PPh_2)_2Pt(PPh_3)$.[25] A similar metal–metal bond plus a trigonal-planar array of ligands is also observed for one of the platinum atoms in the dimeric compound $(Cy_3P)(PhC{\equiv}C)Pt(\mu\text{-}C{\equiv}CPh)(\mu\text{-}SiMe_2)Pt(PCy_3)$.[26] It has been previously suggested that the molecules **1** can best be regarded as containing M(0) and Pt(II) oxidation states (i.e. bonding scheme **5**[18]). For this bonding scheme the M(0) center functions as a Lewis base, giving rise to a dative Mo(0)→Pt(II) interaction. Consistent with this is a ca. 20-cm^{-1} blue shift in the ν(CO) stretching frequency of **1** relative to those of their *cis*-$M(CO)_4(PPh_2H)_2$ analogues. In this regard the

---

(23) Compound **1e**, $C_{34}H_{35}MoO_4P_3Pt$, fw = 891.6, crystallizes as orange-red rhombs/blocks in the orthorhombic space group *Pbca* with $a = 18.381$ (3) Å, $b = 16.989$ (2) Å, $c = 22.462$ (5) Å, $V = 7014$ Å^3, and $D_{calc} = 1.69$ g cm^{-3} for $Z = 8$ with use of Mo Kα radiation, $\lambda = 0.710\,69$ Å, $\mu = 45.4$ cm^{-1}, $F(000) = 3488$, and $T = 298$ K. Unit cell dimensions were based on a least-squares refinement of diffracting positions of 25 reflections ($7.8 < \theta < 15.9°$). Intensity data collection (Enraf-Nonius CAD4 diffractometer, graphite monochromator, ω–2θ scans over $(0.70 + 0.35 \tan\theta)°$, *hkl* quadrant with $2\theta \leq 50°$, maximum scan time of 75 s, and 3 standards every 7500 s) gave 6767 data, including 222 standards (<3% variation in intensity). Lorentz, polarization, and absorption corrections (faces (*d*, cm) {100} (0.0081), {010}, (0.0125), and {001} (0.0150); 8 × 8 × 10 grid; *T* range 0.331–0.502) were applied to all data. Rejecting 896 systematically absent or zero F_o data and averaging 332 symmetry-equivalent data ($R_{merge} = 0.03$) gave 5317 nonzero data. Structure solution: Patterson (Pt + Mo), least-squares, Fourier + ΔF Fourier; H atoms placed in calculated positions. Full-matrix least-squares refinement minimizing $\sum w(\Delta F)^2$ converged (all non-H atoms anisotropic, maximum $\Delta/\sigma = 0.31$) to R (R_w) = 0.0330 (0.0440) for 3225 data with $I \geq 3\sigma(I)$. Weights: $4F^2/[\sigma^2(I) + (0.05F^2)^2]$. The maximum peak in the final ΔF map was 0.89 e Å^{-3}, and $S = 1.125$. Programs: Enraf-Nonius SDP package (B. A. Frenz and Associates, Inc., College Station, TX, 1981) on a PDP 11/23 computer. Scattering factors stored in the program were taken from: *International Tables for X-ray Crystallography*; Kynoch: Birmingham, England, 1974; Vol. IV (present distributor D. Reidel, Dordrecht, The Netherlands).

(24) (a) Bars, O.; Braunstein, P.; Geoffroy, G. L.; Metz, B. *Organometallics* **1986**, *5*, 2021. (b) See Table XX in: Bender, R.; Braunstein, P.; Jud, J. M.; Dusansoy, Y. *Inorg. Chem.* **1984**, *23*, 4489.

(25) Taylor, N. J.; Chieh, P. C.; Carty, A. J. *J. Chem. Soc., Chem. Commun.* **1975**, 448.

(26) Ciriano, M.; Howard, J. A. K.; Spencer, J. L.; Stone, F. G. A.; Wadepohl, H. *J. Chem. Soc., Dalton Trans.* **1979**, 1749.

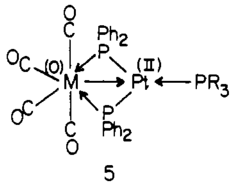

5

complexes 1 are similar to $(OC)_4W(\mu\text{-}PPh_2)_2Ir(H)(CO)(PPh_3)$, for which the arrangement at iridium (ignoring the Ir–W bond) is trigonal bipyramidal (a trigonal-planar arrangement of phosphorus atoms as in 1) and for which a blue shift for ν(CO) of ca. 20 cm^{-1} is also observed.[13] The large $J_{^{195}Pt-^{31}P}$ coupling of ca. 5000 Hz to the PR_3 ligand trans to the Mo→Pt bond (see Table IV) is indicative of a weak trans influence and suggests relatively weak Mo→Pt σ-donation.[27] The large downfield shifts of the μ-PPh_2 ligands ($\delta(P_\mu)$ 170–230 ppm) are typical for metal–metal-bonded systems.[28]

Reaction of $(OC)_4M(\mu\text{-}PPh_2)_2Pt(PR_3)$ with RLi. The complexes 1a–i are, physically and chemically, reasonably robust materials. In a previous paper Geoffroy et al.[18] have described the lack of reactivity of complexes of type 1 with H_2 and CO, their reversible protonation at platinum (using HBF_4), and displacement of PPh_3 from Pt by activated alkynes such as $MeO_2CC{\equiv}CCO_2Me$. Stephan et al.[1] described the synthesis and structural features of $(OC)_4Mo(\mu\text{-}PCy_2)_2M'(PPh_3)$ (M′ = Ni, Pd, Pt) but made no comments concerning their chemical reactivity. However, a reaction of considerable interest involves the reaction of 1 with organolithium reagents. Geoffroy et al.[13] had previously shown that the tungsten–iridium dimer $(OC)_4W(\mu\text{-}PPh_2)_2IrH(CO)(PPh_3)$ (which is structurally very similar to complexes 1) reacts with RLi (R = Me, Ph) to give the lithium acylate/benzoylate 6, which in turn may be alkylated ($Me_3O^+BF_4^-$) to give the methoxycarbene derivatives 7 (eq 5). The reaction of the tricyclohexylphosphine complexes 1f (M = Mo) and 1i (M = W) with a stoichiometric amount of PhLi in THF proceeds according to eq 6 to give the benzoylate complexes $(OC)_3(PhCOLi)M(\mu\text{-}PPh_2)_2Pt(PCy_3)$ (8), isolated as extremely air- and moisture-sensitive orange powders. These complexes were characterized spectroscopically (Tables II and V). Their IR spectra exhibited three ν(CO) bands consistent with a *mer*-$(CO)_3$ arrangement at M. The $^{31}P\{^1H\}$ NMR spectra contained two 1:1:1:1 quartet resonances (plus ^{195}Pt satellites) assignable to nonequivalent μ-phosphido bridges in the region expected for a metal–metal-bonded system[28] together with a quartet assignable to the coordinated PCy_3 (see Table V). The IR and $^{31}P\{^1H\}$ NMR data for 8 are very similar to those previously reported for 6. Methylation of 8 with use of $Me_3O^+BF_4^-$ or CH_3SO_3F gives the phenylmethoxycarbene derivatives $(OC)_3\{PhC(OMe)\}M(\mu\text{-}PPh_2)_2Pt(PCy_3)$ (9). The IR and $^{31}P\{^1H\}$ NMR data of 9 (Tables II and V) are similar to those of 7 and confirm the structure shown with the carbene trans to a μ-PPh_2 ligand. The large $J_{^{195}Pt-^{31}P}$ coupling of ca. 5000 Hz to the PCy_3 ligand in 8 and 9 is indicative of relatively weak M→Pt σ-donation as observed in 1.

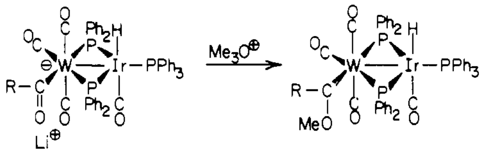

(5)

6 7

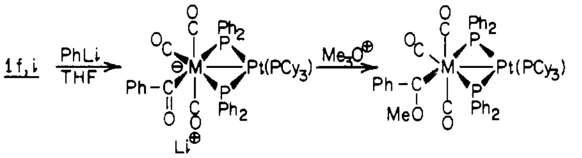

(6)

8f M=Mo 9f M=Mo
8i M=W 9i M=W

The PPh_3 complexes (M = Mo (1d), W (1g)) react with PhLi in THF to give mainly the benzoylate (8d,g; ca. 80%) together with a small amount of the phenylplatinum complex $[(OC)_4M(\mu\text{-}PPh_2)_2PtPh(PPh_3)]Li$ (10d,g; ca. 20%). The corresponding chromium PPh_3 complex 1a reacts with PhLi in THF to give the phenylplatinum derivative 10a as the sole product. The proposed structure of 10 is based primarily on the $^{31}P\{^1H\}$ NMR data (Table VII). Three ^{31}P resonances are observed with the chemical shifts of the two μ-phosphido ligands being in the region expected for systems *without* metal–metal bonds.[28] When the solvent is changed from THF to benzene, the complexes 1 (PR_3 = PEt_3, PPh_3) react with PhLi to give 10 as the sole product, while the PCy_3 complexes 1c,f,i exhibit *no reactivity* toward PhLi in benzene. The tendency to form the phenylplatinum derivative 10 is presumably influenced by the steric bulk of the coordinated PR_3 (i.e. PEt_3 > PPh_3 ≫ PCy_3 (no Ph–Pt product formed)), while formation of the benzoylate is more favored for Mo and W relative to Cr and is also favored by the use of THF vs benzene as solvent. The reason for the effect of the solvent on site preference for PhLi addition is not clear but may be due to differences in ion-pairing effects. Reaction of 1f with the hydride donor $LiAlH_4$ or $NaBH_4$ gave the hydridoplatinum complex 11, characterized in solution by ^1H and $^{31}P\{^1H\}$ NMR spectroscopy (see Table V). No evidence of a formylate species, structurally similar to 8, was obtained.

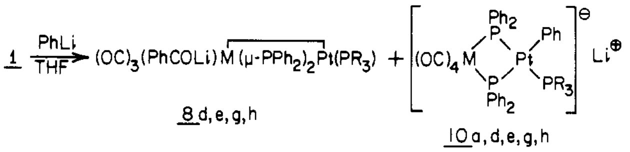

8d,e,g,h 10a,d,e,g,h

(7)

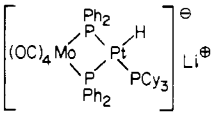

11

Addition of excess PhLi to $(OC)_4M(\mu\text{-}PPh_2)_2Pt(PR_3)$ (PR_3 = PEt_3, PPh_3) in benzene results in the displacement of the PR_3 group and the formation of the dianionic species $[(OC)_4M(\mu\text{-}PPh_2)_2Pt(Ph)_2]Li_2$ (12) (eq 8). Support for this structure is based solely on $^{31}P\{^1H\}$ NMR solution studies, which show a singlet resonance assignable to the free phosphine (PEt_3 or PPh_3) together with a 1:4:1 triplet in the region expected for phosphido bridges in non-metal–metal-bonded systems. The value of $J_{^{195}Pt-^{31}P}$ (ca. 1300 Hz) is consistent with P_μ being trans to Ph (a strong σ-donor with a large trans influence). The dianion 12 is more readily formed from the PPh_3 systems, consistent with the expected ease of displacement PPh_3 > PEt_3.

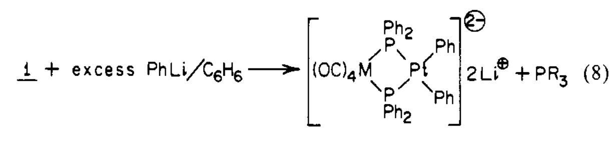

(8)

12 (M=Cr, Mo, W)

Discussion

Complexes of the type $(OC)_4M(\mu\text{-}PPh_2)_2M'L_x$ (M = Cr, Mo, W) will react with RLi to give the acylate/benzoylate products $(OC)_3(RCOLi)M(\mu\text{-}PPh_2)_2M'L_x$. Besides the reaction of 1 to give 8 and that of $(OC)_4W(\mu\text{-}PPh_2)_2IrH(CO)(PPh_3)$ to give 6[13] (see above), other examples include $(OC)_4W(\mu\text{-}PPh_2)_2Re(CO)_3Me$ to give $(OC)_3(RCOLi)W(\mu\text{-}PPh_2)_2Re(CO)_3Me$[10] and

---

(27) Appleton, T. G.; Clark, H. C.; Manzer, L. E. *Coord. Chem. Rev.* **1973**, *10*, 335.

(28) (a) Peterson, J. L.; Stewart, R. P., Jr. *Inorg. Chem.* **1980**, *19*, 186. (b) Carty, A. J.; MacLaughlin, S. A.; Taylor, N. J. *J. Organomet. Chem.* **1981**, *204*, C27. (c) Carty, A. J. *Catalytic Aspects of Metal Phosphine Complexes*; Advances in Chemistry 196; American Chemical Society: Washington, DC, 1982; p 163.

Table V. $^{31}P\{^1H\}$ NMR Data for Complexes **8–12**[a]

	M	R	$\delta_{P_\mu{}^a}$	$\delta_{P_\mu{}^b}$	δ_{P^c}	$J_{^{31}P^a-^{31}P^b}$	$J_{^{31}P^b-^{31}P^c}$	$J_{^{31}P^a-^{31}P^c}$	$J_{^{195}Pt-^{31}P^a}$	$J_{^{195}Pt-^{31}P^b}$	$J_{^{195}Pt-^{31}P^c}$	$J_{^{183}W-^{31}P^{a,b}}$
8c	Cr	Cy	207	175	66	195	20	70	3020	2635	5000	
8d	Mo	Ph	185	144	50	165	12	78	3000	2385	5040	
8e	Mo	Et	193	148	37	170	11	78	2800	2300	4900	
8f	Mo	Cy	191	146	63	183	12	76	2968	2435	4888	
8g	W	Ph	151	118	50	180	12	63	2866	2292	5022	not res
8h	W	Et	158	141	37	189	16	64	not res			
8i	W	Cy	157	121	62	198	11	61	2835	2430	4864	199, 189
9f	Mo	Cy	200	164	64	187	10	73	2914	2408	4876	
9i	W	Cy	196	143	78	209	10	56	2856	2314	4673	199, 200
10a	Cr	Ph	−55	−90	19	45	15	300	2000	1200	2176	
10b	Cr	Et	−71	−92	7.5	45	17	282	1880	1200	2200	
10d	Mo	Ph	−81	−102	7	0	15	270	1880	1260	2000	
10e	Mo	Et	−79	−98	7	0	11	295	1735	1124	2058	
10g	W	Ph	−87	−99	24	0	13	299	1925	1283	not res	not res
10h	W	Et	−102	−132	9	10	13	301	1872	1137	2243	not res
11[b]	Mo	Cy	−68	−92	40	8	7	266	1820	1230	2243	
12	Cr		−80						1320			
12	Mo		−90						1278			
12	W		−112						1370			214

[a] $P_\mu{}^a$ is trans to PhCOY (Y = Li, Me); $P_\mu{}^b$ is trans to CO. δ values are in ppm and J values in Hz; res = resolved. [b] ^1H NMR data for $[(OC)_4Mo(\mu\text{-}PPh_2)_2PtH(PCy_3)]^-Li^+$ (**11**), hydrido region: $\delta_H = -7.45$; $J_{^{195}Pt-^1H} = 1000$; $J_{^{31}P-^1H} = 140, 11, 7$.

Table VI. Electronic Distribution at the Carbon Atoms in the LUMO

	$(H_3P)Pt\text{-}(\mu\text{-}PH_2)_2Mo(CO)_4$ (**15**)	$(OC)_4Mo\text{-}(\mu\text{-}PH_2)_2Mo(CO)_4$ (**16**)	$(OC)_4Mo(PH_3)_2$ (**17**)
ax. CO	0.06	0.03	0.75
eq CO	0.13	0.14	0.02

Table VII. Net Charge for the Axial and Equatorial Carbonyl Ligand C Atoms for the Metallic Fragments and Complete Molecules

frag/molecule	ax. CO	eq CO
$(H_3P)Mo(CO)_4$	0.70	0.68
$(H_3P)Pt(\mu\text{-}PH_2)_2Mo(CO)_4$	0.71	0.76
$(OC)_4MoMo(CO)_4$	0.71	0.68
$(OC)_4Mo(\mu\text{-}PH_2)_2Mo(CO)_4$	0.72	0.78
$(OC)_4Mo$	0.73	0.66
$(OC)_4Mo(PH_3)_2$	0.73	0.67

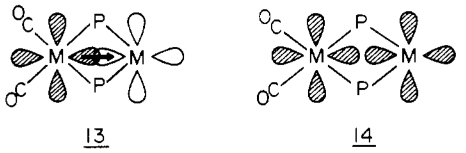

Figure 2. Simplified bonding scheme illustrating the effect of M–Pt bonding on M–CO bonding trans to P_μ.

$(OC)_4\overline{M(\mu\text{-}PPh_2)_2M}(CO)_4$ (M = Mo, W) to give $(OC)_3(RCOLi)\overline{M(\mu\text{-}PPh_2)_2M}(CO)_4$.[20] This last compound can also be obtained from $[(OC)_4W(\mu\text{-}PPh_2)_2W(CO)_4]^{2-}$ and R^+. This observed reactivity is of 2-fold interest: (i) Acylates/carbenes are not obtained from the reaction of RLi with *cis*-$M(CO)_4(PR_3)_2$ (M = Cr, Mo, W).[19] No isolable product was obtained from the reaction of RLi with $(OC)_4W(\mu\text{-}PPh_2)_2ZrCp_2$,[3] while the reactivity of $(OC)_4Mo(\mu\text{-}PEt_2)_2HfCp_2$ toward RLi was not given.[4] (These are compounds with no, or only very weak, metal–metal bonds.) (ii) Upon reaction of RLi with $M(CO)_5(PR_3)$[19] and with the crown-ether-containing system *cis*-$(OC)_4M(Ph_2POCH_2CH_2OCH_2\text{-})_2$ (M = Cr, Mo, W)[29] (where the reaction is favored by preferential complexation of Li^+ by the acylate product) the resulting acylates and/or benzoylates (and subsequent carbene derivatives) are coordinated trans to a CO ligand rather than trans to a P-donor ligand, as is the case in $(OC)_3(RCOLi)\overline{M(\mu\text{-}PPh_2)_2M'}L_x$ products (i.e. the formation of $(OC)_3(RCOLi)\overline{M(\mu\text{-}PPh_2)_2M'}L_x$ (a) appears to be an exception to the general observation that in octahedral systems a CO trans to CO is more susceptible to nucleophilic addition at carbon than a CO trans to PR_3[19,30] and (b) implies some additional CO activation parameter in $(OC)_4\overline{M(\mu\text{-}PPh_2)_2M'}L_x$ vis à vis *cis*-$M(CO)_4(PR_3)_2$ complexes, which are unreactive toward RLi reagents).[19] *A qualitative rationale* for points i and ii above can be obtained from consideration of the two simple bonding representations **13** and **14** for systems with and without a metal–metal bond, respectively (Figure 2). If one assumes that a filled d_{xy} orbital of M is involved to a significant extent in a direct M→M′ dative bond in **13**, then the net result will be a decrease in $d_{xy} \rightarrow \pi^*$ CO bonding to the equatorial CO's (trans to P) such that these CO's should be more susceptible to nucleophilic addition at C vis à vis the equatorial CO's of **14**. In the case of $(OC)_4\overline{M(\mu\text{-}PR_2)_2M}(CO)_4$ the M–M bond arises from overlap of the two d_{xy} orbitals (two electrons) which also exhibit a π-interaction with four equatorial CO's as opposed to two electrons (filled d_{xy})/2 equatorial CO's in $M(CO)_4(PR_3)_2$.

Reactivity of $(OC)_4\overline{Mo(\mu\text{-}PH_2)_2Pt}(PH_3)$ toward Nucleophiles: Extended Hückel MO Calculation. As a further approach to the rationalization of the regiospecificity of the nucleophilic attack (see above), the three simplified complexes $(OC)_4\overline{Mo(\mu\text{-}PH_2)_2Pt}(PH_3)$ (**15**), $(CO)_4\overline{Mo(\mu\text{-}PH_2)_2Mo}(CO)_4$ (**16**), and *cis*-$Mo(CO)_4(PH_3)_2$ (**17**) were studied by using extended Hückel molecular orbital calculations and the fragment orbital formalism.[31] The last two complexes, **16** and **17**, were computed for comparative purposes. Complex **16** was chosen because of its similar reactivity[20] toward nucleophiles (i.e., the same as for **1**, although it was previously suggested that the nucleophilic attack occurred at the equatorial CO because of a steric effect). While complexes of the type **17** are unreactive toward RLi, it is predicted that the reversed regiospecificity[30] (i.e. nucleophilic attack occurring at the axial CO trans to a CO group) should be preferred, as observed in $M(CO)_5(PR_3)$. Calculations on **17** will be used as a reference. It is worth noting that d orbitals on the phosphorus atoms were not included in the calculations, which is in agreement with the conclusion[32] obtained by ab initio calculations that d orbitals on phosphorus are not necessary for a qualitative understanding of back-bonding effects.

According to the calculations, it appears that the nucleophilic attack at the carbon of the carbonyl ligand may be considered

---

[29] Powell, J.; Kuksis, A.; May, C. J.; Smith, S. G.; Nyburg, S. C. *J. Am. Chem. Soc.* **1981**, *103*, 5941.

[30] Darensbourg, M. Y.; Hankel, J. M. *Organometallics* **1982**, *1*, 82.

[31] (a) Hoffmann, R. *J. Chem. Phys.* **1963**, *39*, 1397. (b) Hoffmann, R.; Lipscomb, W. *J. Chem. Phys.* **1962**, *36*, 2179. (c) Hoffmann, R.; Lipscomb, W. *J. Chem. Phys.* **1962**, *37*, 2872.

[32] Marynick, D. S. *J. Am. Chem. Soc.* **1984**, *106*, 4064.

Table VIII. Selected Metal–Ligand Bond Length and Bond Angle Data for Complexes of the Type $(OC)_4\overline{M(\mu\text{-}PR_2)_2M'}L_x$ and *cis*-$(OC)_4M(PR_3)_2$

compd	av M–P, Å	∠PMP, deg	av M–C trans to P, Å	av M–C cis to P, Å	∠MPM′, deg	M–M′, Å	∠CMC trans to P_2, deg
$(OC)_4\overline{Mo(\mu\text{-}PPh_2)_2Pt}(PEt_3)$ (**1e**)	2.506 (3)	100.6 (1)	2.014 (11)	2.023 (11)	70.8 (1)	2.766 (1)	95.0 (4)
$(OC)_4\overline{W(\mu\text{-}PPh_2)_2Pt}(PPh_3)$ (**1g**)[18]	2.508 (4)	100.8 (1)	1.996 (14)	2.008 (14)	70.7 (1)	2.764 (1)	89.9 (5)
$(OC)_4\overline{W(\mu\text{-}PPh_2)_2Pt}(MeO_2CC{\equiv}CCO_2Me)$[18]	2.439 (3)	102.2 (1)	2.021 (12)	2.041 (12)	72.4 (1)	2.795 (1)	86.3 (4)
$(OC)_4Mo(\mu\text{-}PEt_2)_2HfCp_2$[4]	2.536 (1)	98.2 (1)	1.987 (4)	2.038 (4)	83.0 (1)	3.400 (1)	89.1 (2)
$(OC)_4W(\mu\text{-}PPh_2)_2ZrCp_2$[3]	2.533 (3)	103.3 (1)	1.983 (14)	2.006 (14)	79.2 (1)	3.289 (1)	86.0 (5)
cis-$(OC)_4Mo(PMe_3)_2$[29]	2.522 (1)	97.5 (1)	1.971 (6)	2.032 (14)			88.2 (2)
cis-$(OC)_4Mo(PEt_3)_2$[29]	2.544 (4)	100.3 (1)	1.977 (1)	2.032 (5)			85.3 (2)
cis-$(OC)_4Mo(PPh_3)_2$[29]	2.577 (2)	104.6 (1)	1.972 (2)	2.040 (19)			83.0 (3)
$(OC)_4\overline{W(\mu\text{-}PPh_2)_2Ir}H(CO)(PPh_3)$[13]	2.531 (2)	99.8 (1)	2.006 (9)	2.029 (7)	72.8 (1)	2.8764 (6)	89.8 (3)
$(OC)_3\{C(OCH_3)Ph\}\overline{W(\mu\text{-}PPh_2)_2Ir}H(CO)(PPh_3)$[13]	2.501 (5)	100.9 (2)	1.90 (2) 2.02 (2)[a]	2.01 (2)	72.8 (1)	2.858 (1)	85.2 (8)[a]
$(OC)_4\overline{W(\mu\text{-}PPh_2)_2Re}(CO)_3Me$[10]	2.474 (3)	102.1 (1)	2.042 (15)	2.011 (15)	76.1 (1)	3.015 (1)	88.2 (6)
$(OC)_4\overline{W(\mu\text{-}PPh_2)_2Ir}(H)(COD)$[7]	2.505 (6)	99.0 (2)	1.99 (2)	2.06 (2)	73.9 (2)	2.893 (1)	88 (1)

[a] Data for carbene ligand.

to be *frontier orbital* and *charge controlled.* Table VI contains the electronic distribution at the carbon atoms of the carbonyl ligands for the LUMO of each of the three complexes. It can be seen that the experimentally observed regiospecificity of RLi addition to **1** correlates well with the magnitude of the charge distribution for both available sites in the LUMO. The two complexes containing phosphido bridges, **15** and **16**, have a higher charge in the equatorial (i.e. trans to the phosphorus) CO's than in the axial CO's and vice versa for the cis-phosphine complex **17**. Figure 3 shows the electron density plot for the LUMO of complex **15** in two different planes (the *xy* plane contains the equatorial CO and the *xz* plane contains the axial CO's) and is consistent with preferred attack (if frontier orbital controlled) at the equatorial carbonyl. The regiospecificity of the nucleophilic attack also correlates with the electropositive character at the carbon atom of the carbonyl ligand. Table VII shows the net charge for both axial and equatorial carbons of the CO's for the complete molecules, and to emphasize the effect of the phosphido bridges, the net charges are also presented for the metallic fragments without the bridging ligands.[33] In the monomer **17**, the axial carbons are far more electropositive than those trans to the PH_3 ligands; it can also be seen that adding two phosphine ligands to the $Mo(CO)_4$ fragment slightly depletes the trans carbons of their electron density. The situation is reversed when phosphido bridges are trans to the CO's (i.e. **15** and **16**). The equatorial carbon atoms are then more electropositive. The effect of adding the phosphido bridges to the metallic fragments is an increase in the electropositivity of the equatorial carbons of **16** of about 12–15%, while that of the carbons of the axial CO's remains unchanged. It should also be noted that the LUMO's of **15** (Figure 2) and **16** are antibonding with respect to MoPt/MoMo. Addition of PhLi to **1** (PR_3 = PEt_3, PPh_3) in C_6H_6 gave $[(OC)_4M(\mu\text{-}PPh_2)_2PtPh(PR_3)]^-$ (no M–Pt bond). Similarly, $[(OC)_4M(\mu\text{-}PPh_2)_2M(CO)_4]^{2-}$ has a nonbonded M- - -M situation.[20,34] In contrast, the negative charge brought up by the Ph^- anion in the formation of $(OC)_3(PhCOLi)\overline{M(\mu\text{-}PPh_2)_2Pt}(PR_3)$ is not distributed all over the complex; rather, it is localized on the more electronegative oxygen of the benzoylate ligand. (Calculations were performed on $[(OC)_3(HCO)\overline{Mo(PH_2)_2Pt}(PH_3)]^-$. A similar result was presented from ab initio calculations on the complex $[Fe(CO)_4(HCO)]^-$.[35])

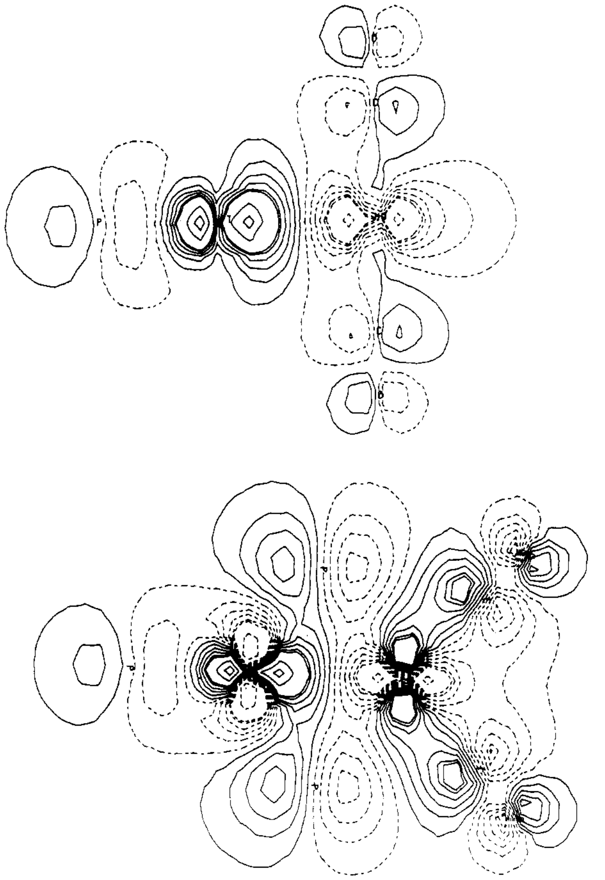

Figure 3. Electron density plot for the LUMO of the model compound $(OC)_4\overline{Mo(\mu\text{-}PH_2)_2Pt}(PH_3)$ (**15**): (a) in the *xz* plane, axial CO's; (b) in the *xy* plane, equatorial CO's ($Mo(CO)_4$ unit on the right).

Structural Comparisons of $(OC)_4\overline{M(\mu\text{-}PPh_2)_2M'}L_x$, $(OC)_4M(\mu\text{-}PPh_2)_2M'L_y$, and *cis*-$M(CO)_4(PR_3)_2$. Recent structural studies of several "$(OC)_4M$"-containing bis(phosphido) heterobimetallic systems now allow for a comparison of the structural features of the $(OC)_4MP_2$ unit vis à vis metal–metal bonding vs no metal–metal bond and for *cis*-$M(CO)_4(PR_3)_2$ situations. A comparison of some of the structural features of **1e** and other $(OC)_4\overline{M(\mu\text{-}PR_2)_2M'}L_x$ systems with metal–metal bonds ($M'L_x$ = $Pt(PPh_3)$, $Pt(MeO_2CC{\equiv}CCO_2Me)$,[18] $IrH(CO)(PPh_3)$,[13] $IrH(COD)$,[7] $Re(CO)_3Me$[10]) with those of bis(phosphido)-bridged systems that contain no, or very weak, metal–metal bonds (e.g. $(OC)_4Mo(\mu\text{-}PEt_2)_2HfCp_2$[4] and $(OC)_4W(\mu\text{-}PPh_2)_2ZrCp_2$[3]) and with those of *cis*-$Mo(CO)_4(PR_3)_2$ (R = Me, Et, Ph)[36] is given in Table VIII.

---

(33) Elian, M.; Hoffmann, R. *Inorg. Chem.* **1975**, *14*, 1058.

(34) Keiter, R. L.; Madigan, M. J. *Organometallics* **1982**, *1*, 409.

(35) Dedieu, A.; Nakamura, S. *Nouv. J. Chim.* **1984**, *8*, 317.

(36) Cotton, F. A.; Darensbourg, D. J.; Klein, S.; Kolthammer, B. W. S. *Inorg. Chem.* **1982**, *21*, 2661.

(The increase in average Mo–P bond length of *cis*-$Mo(CO)_4(PR_3)_2$ ($PMe_3 < PEt_3 < PPh_3$) has been ascribed to steric effects.[36]) As previously observed and commented on for *cis*-$M(CO)_4(PR_3)_2$ systems, the two types of carbonyl ligands in these compounds have different M–C distances. Those trans to a P-donor ligand (PR_3 or μ-PR_2) are closer to the metal center than those trans to CO. The P–M–P bond angle in all of the phosphido bridge systems, in the range 98–103°, is very similar to those observed in *cis*-$Mo(CO)_4(PR_3)_2$. The most noticable difference is to be found in the M–P bond distances. While the average M–P distances in $(OC)_4Mo(\mu\text{-}PEt_2)_2HfCp_2$ (2.536 (1) Å) and $(OC)_4W(\mu\text{-}PPh_2)_2ZrCp_2$ (2.533 (3) Å) (no or very weak metal–metal bonds) are comparable to the values observed in *cis*-$Mo(CO)_4(PR_3)_2$, the average M–P distances observed in the metal–metal-bonded systems **1e** (2.506 (3) Å), **1g** (2.508 (4) Å), and $(OC)_4W(\mu\text{-}PPh_2)_2Pt(MeO_2CC{\equiv}CCO_2Me)$ (2.433 (3) Å) are significantly shorter. The reported average W–P bond length for the iridium system $(OC)_4W(\mu\text{-}PPh_2)_2IrH(CO)(PPh_3)$ (2.531 (2) Å) is somewhat longer than is observed for the M→Pt-bonded systems. However, the iridium–tungsten carbene system $(OC)_3\{C(OMe)Ph\}W(\mu\text{-}PPh_2)_2IrH(CO)(PPh_3)$ has an average W–P distance (2.501 (5) Å) that is likewise indicative of a significant shortening of the M–P bond in these metal–metal-bonded systems. We have previously commented on a similar shortening of the Mn–P_μ bond length in systems containing the "-$(OC)_4Mn(\mu\text{-}PR_2)$" unit on going from systems with no metal–metal bonds, to systems with a hydride bridge, to systems with "Mn–M" bonds[37] (e.g. $[(OC)_4Mn(\mu\text{-}PH_2)]_2$, average Mn–$P_\mu$ = 2.351 (2) Å, ∠MnPMn = 104°; $[(OC)_4Mn(\mu\text{-}PPh_2)(\mu\text{-}H)Mn(CO)_4]$, average Mn–$P_\mu$ = 2.294 (6) Å, ∠MnPMn = 80°; $[(OC)_4Mn(\mu\text{-}PPh_2)Fe(CO)_4]$, Mn–$P_\mu$ = 2.257 (6) Å, ∠MnPFe = 78°). Likewise, as one goes from $(OC)_5W(\mu\text{-}PPh_2)OsH(CO)_2(PPh_2H)(PPh_2Me)$[11] (no W–Os bond) to $(OC)_4W(\mu\text{-}PPh_2)(\mu\text{-}Ph_2PCHOMe)Os(CO)_2(PPh_2Me)$[8] (W–Os bond), W–$\mu$-$PPh_2$ decreases from 2.623 (2) to 2.538 (3) Å, Os–μ-PPh_2 decreases from 2.478 (2) to 2.357 (7) Å, and ∠WPOs decreases from 116 to 76°. We have previously suggested that this consistent shortening of M–P_μ on going to metal–metal-bonded systems is a consequence of ring strain effects and bent M–P σ-bonding in systems with acute MPM′ angles.[37,38] In this latter respect it should be noted that (i) the large deviations of PPtP angles from 90 or 180° ideal values in "planar" $PtXY(PR_3)_2$ complexes have recently been rationalized reasonably successfully in terms of R_3P–Pt bond bending,[39] (ii) the shortening of the P–P bond in P_4 (2.21 Å) relative to a typical P–P bond length in unstrained systems (2.27 Å) has been attributed to bent σ-bonding involving p-orbital overlap rather than d–d π-bonding,[42] and (iii) the one-bond coupling $^1J_{^{195}Pt-^{31}P}$, in the cationic complexes $[Cp(ON)Re(H)(\mu\text{-}PPh_2)Pt(PPh_3)_2]^+$, is ca. 50% smaller for μ-PR_2 vis â vis that for a PPh_3 ligand with a comparable P–Pt bond length, consistent with a reduced P 3s orbital contribution to the P_μ–Pt bond.[38] In complex **1e** the P–Pt bond lengths are very similar (within 0.02 Å) yet $^1J_{^{195}Pt-^{31}P_\mu}$ (2718 Hz) is considerably smaller than $^1J_{^{195}Pt-^{31}PEt_3}$ (4938 Hz), consistent with less P 3s character in the P_μ–Pt bond.

Experimental Section

General Considerations. All manipulations were carried out under an atmosphere of dry N_2 using dry degassed solvents. Phosphorus and proton NMR spectra were recorded as CD_2Cl_2 solutions at room temperature on a Varian XL200 FTNMR spectrometer operating at 80.9 and 200 MHz, respectively. Proton shifts were measured relative to TMS. Phosphorus shifts were measured relative to external $P(OMe)_3$ in C_6D_6 and corrected to 85% H_3PO_4, with downfield shifts reported as positive. Infrared data were obtained on a Nicolet 10DX FTIR spectrometer. Samples were run as CH_2Cl_2 solutions in sodium chloride cells.

Starting Materials. Deuteriodichloromethane was purchased from Aldrich and used as received. Metal carbonyl starting materials were purchased from Strem and Pressure Chemicals and used without further purification. Diphenylphosphine was purchased from Pressure Chemicals. The compounds *cis*-$PtCl_2(PEt_3)_2$,[41] $Pt(C_2H_4)(PPh_3)_2$,[42] $Pt(C_2H_4)_2(PCy_3)$,[43] $(OC)_4M(\mu\text{-}PPh_2)(\mu\text{-}H)Pt(PPh_3)_2$,[22] and $(OC)_4M(\mu\text{-}PPh_2)(\mu\text{-}H)Pt(CO)(PCy_3)$[22] were prepared according to published procedures. The secondary phosphine complexes $M(CO)_5(PPh_2H)$ and $M(CO)_4(PPh_2H)_2$ were prepared from $Et_4N[M(CO)_5Cl]$ and PPh_2H by following the procedure given for the synthesis of $M(CO)_5(PR_3)$ and $M(CO)_4(PR_3)_2$.[45]

Preparation of $(OC)_4Mo(\mu\text{-}PPh_2)_2Pt(PEt_3)$ (1e) (Eq 2). PhLi (1.7 M, 3.3 mL, 5.6 mmol) in cyclohexane/diethyl ether (70/30) was added via syringe to a THF solution (30 mL) of $Mo(CO)_5(PPh_2H)$ (2.36 g, 5.6 mmol) and *cis*-$PtCl_2(PEt_3)_2$ (1.38 g, 2.76 mmol). The resultant orange solution was allowed to stand at room temperature overnight. The solvent was removed under vacuum and the remaining brown oil extracted with hexane (10 × 15 mL) to remove PEt_3. Chromatography (Florisil column with 10% CH_2Cl_2/90% hexane as eluant) gave an orange band containing **1e** isolated in 16% yield (0.39 g, 0.44 mmol). **1e** was recrystallized from CH_2Cl_2/pentane. The complexes **1b** and **1h** were likewise prepared with a similar yield.

Preparation of 1e from *cis*-$(OC)_4Mo(PPh_2Li)_2$ and *cis*-$PtCl_2(PEt_3)_2$ (eq 1) in THF gave a 40% overall yield of **1e**.

Preparation of $(OC)_4Cr(\mu\text{-}PPh_2)_2Pt(PPh_3)$ (1a) (Eq 3). PPh_2H (0.17 mL, 0.98 mmol) was added via syringe to a CH_2Cl_2 solution (10 mL) of $(OC)_4Cr(\mu\text{-}H)(\mu\text{-}PPh_2)Pt(PPh_3)_2$ (1.05 g, 0.98 mmol). The resultant yellow solution was stirred for 30 min, the solvent removed, and the product extracted with hexane (3 × 25 mL) to remove PPh_3. The remaining yellow solid, $(OC)_4Cr(\mu\text{-}H)(\mu\text{-}PPh_2)Pt(PPh_3)(PPh_2H)$ (**3a**), was refluxed in toluene (25 mL) for 2 h to drive off H_2. The orange solid remaining after removal of solvent was recrystallized from CH_2Cl_2/pentane to give a 78% yield of **1a** (0.76 g, 0.76 mmol). Identical procedures gave **1e** (76% yield) and **1g** (75% yield).

Preparation of $(OC)_4Cr(\mu\text{-}PPh_2)_2Pt(PCy_3)$ (1c) (Eq 4). PPh_2H (0.22 mL, 1.26 mmol) was added to a toluene solution of $(OC)_4Cr(\mu\text{-}H)(\mu\text{-}PPh_2)Pt(CO)(PCy_3)$ (1.08 g, 1.26 mmol). The resulting solution was refluxed for 2 h to eliminate H_2. The orange solid remaining after removal of solvent was recrystallized from CH_2Cl_2/pentane to give **1c** in 80% yield (1.00 g, 0.99 mmol). An identical procedure gave **1f** (50%) and **1i** (37%).

Preparation of 1f from *cis*-$Mo(CO)_4(PPh_2H)_2$ (Eq 4). *cis*-$Mo(CO)_4(PPh_2H)_2$ (1.09 g, 1.88 mmol) was added to $Pt(C_2H_4)_2(PCy_3)$ (0.99 g, 1.88 mmol) in CH_2Cl_2 (10 mL). After 1 h addition of pentane precipitated $(OC)_4Mo(\mu\text{-}H)(\mu\text{-}PPh_2)Pt(PCy_3)(PPh_2H)$ (**3b**) in 88% yield. Redissolving **3b** in toluene and refluxing for 2 h gave, on workup, orange crystals (from CH_2Cl_2/pentane) of **1f** (90% yield). Complex **1i** was similarly prepared in 90% overall yield from $(OC)_4W(PPh_2H)_2$ and $Pt(C_2H_4)_2(PCy_3)$.

Preparation of $[Li(THF)_x][(OC)_3\{C(O)Ph\}Mo(\mu\text{-}PPh_2)_2Pt(PCy_3)]$ (8f). PhLi (1.5 M, 0.49 mL, 0.742 mmol) was added via syringe to a THF (10 mL) solution of **1f**. The solution was stirred for 20 min and the solvent reduced to 2 mL (in vacuo). Benzene (20 mL) was added, and **8f** precipitated as an orange powder. The highly air-sensitive product was washed with benzene (3 × 5 mL) and dried in vacuo to give **8f** (0.76 g, 0.67 mmol, 90% yield). The tungsten analogue **8i** was similarly prepared.

Preparation of $[(OC)_3\{C(OMe)Ph\}Mo(\mu\text{-}PPh_2)_2Pt(PCy_3)]$ (9f). CH_3SO_3F (0.15 mL, 1.86 mmol) was added via syringe to an acetone (5 mL) solution of **8f** (0.76 g, 0.66 mmol). The solution was stirred for 20 min and the solvent removed (in vacuo). The remaining purple oil was extracted with hexane (3 × 25 mL). Removal of the hexane gave **9f** (0.60 g, 0.525 mmol, 70% yield) as a purple solid. **9f** decomposes in the presence of moisture to form **1f**, benzaldehyde, and other unidentified products. Anal. Calcd (Found) for $C_{53}H_{61}MoO_4P_3Pt$: C, 55.55 (55.86); H, 5.32 (5.61). The tungsten analogue **9i** was likewise isolated as a purple solid (70% yield).

Reactions of the Complexes 1a–i with PhLi (NMR Monitoring). PhLi was added via syringe to either a THF (3 mL) or C_6H_6 (3 mL) solution of **1** in an NMR tube fitted with a rubber septum and C_6D_6 insert. The

---

(37) Powell, J.; Sawyer, J. F.; Shiralian, M. *Organometallics* **1989**, *8*, 577.

(38) Powell, J.; Sawyer, J. F.; Stainer, M. V. R. *Inorg. Chem.*, in press.

(39) Powell, J. *J. Chem. Soc., Chem. Commun.* **1989**, 200.

(40) Hilliar, I. A.; Saimders, V. R. *J. Chem. Soc. D* **1970**, 1233.

(41) Parshall, G. W. *Inorg. Synth.* **1969**, *12*, 27.

(42) Blake, D. M.; Roundhill, D. M. *Inorg. Synth.* **1978**, *18*, 120.

(43) Spencer, J. L. *Inorg. Synth.* **1979**, *19*, 216.

(44) Reference deleted in proof.

(45) Schenk, W. A.; *J. Organomet. Chem.* **1979**, *179*, 253.

resultant products **8**, **10**, and **12**, with the exception of **8f** and **8i** (see above), were not isolated and were characterized on the basis of ^{31}P NMR data (see Table V).

EHMO calculations[31,33] were carried out on the simplified complexes $(OC)_4\overline{Mo(\mu\text{-}PH_2)_2Pt}(PH_3)$ (**15**), $(CO)_4\overline{Mo(\mu\text{-}PH_2)_2Mo}(CO)_4$ (**16**), and *cis*-$(CO)_4Mo(PH_3)_2$ (**17**) with interatomic distances based on X-ray crystal structure determinations[36,46] with idealized geometries: C_{2v} for **15**, D_{2h} for **16**, and C_{2v} for **17**. The P-H distances were 1.40 Å and ∠MPH = 110° for the PH_3 group, and ∠HPH = 109° for PH_2 groups. Variation of ∠HPH from 109 to 120° did not significantly change the observed trends. Values for H_{ii} and orbital exponents were taken from ref 47.

The formyl complex $[(OC)_3(HCO)\overline{Mo(PH_2)_2Pt}(PH_3)]^-$ was calculated with C—H = 0.95 Å, C═O = 1.33 Å, and ∠MoCH = 117°. The CHO group was rotated around the Mo–C vector in order to find the minimum energy configuration.

Acknowledgment. We thank the Natural Sciences and Engineering Research Council of Canada for financial support of this work.

Supplementary Material Available: Tables SI–SIV, containing final atomic and thermal parameters of the hydrogen atoms, general temperature factor expressions, bond distances, and bond angles (5 pages); Table SV, containing observed and calculated final structure factors (27 pages). Ordering information is given on any current masthead page.

---

(46) Link, M. H.; Nassinbeni, L. R. *Inorg. Nucl. Chem. Lett.* **1973**, *9*, 1105.

(47) Summerville, R. H.; Hoffmann, R. *J. Am. Chem. Soc.* **1976**, *98*, 7240.

Contribution from the Chemistry Department, Yale University,
225 Prospect Street, New Haven, Connecticut 06511

Thermal and Photochemical C-H Bond Reactions of Alkenes in (Tris(pyrazolyl)borato)iridium(I) Complexes

Robin S. Tanke and Robert H. Crabtree*

Received March 30, 1989

$[Ir(ol)_2Cl]_2$ (ol = cyclooctene or ethylene) reacts with KTp (Tp = hydrotris(1-pyrazolyl)borate) to give, in the cyclooctene case, TpIr(η^3-cyclooctenyl)H (**1**) and, in the ethylene case, $TpIr(C_2H_4)_2$ (**2**). Complex **2** reacts with CO at 1 atm and 25 °C to give the known $TpIr(CO)_2$ (**3**) and reacts with excess methyl acrylate (MA) to give $TpIr(C_2H_4)(MA)$ (**5**). On irradiation (350 nm), **2** gives TpIr(η^2-C_2H_4)H(η^1-vinyl) (**4**). This appears to take place by intramolecular vinyl C–H bond activation; η^3-$TpIr(C_2H_4)$ is proposed as the key intermediate. In the ^1H NMR spectrum, the ethylene ligands of **2** show a singlet at room temperature for the vinylic protons, but decoalescence takes place at ca. 260 K ($\Delta G_{rot}^{\ddagger}$ = 13 kcal/mol).

Introduction

Tp complexes (Tp = hydrotris(1-pyrazolyl)borate) were first prepared by Trofimenko[1] in the 1960s, but a number of new applications have only very recently appeared. Graham[2] has shown that compounds of the type Tp*M(CO)$_2$ (M = Ir, Rh; Tp* = hydrotris(3,5-dimethyl-1-pyrazolyl)borate) activate alkanes (RH) on irradiation at 350 nm to give Tp*M(CO)H(R). Work in our own group on alkane activation[3] has involved a search for degradation-resistant ligands. We wondered whether Tp or Tp* might be suitable and so set out to make examples of polyhydrides, $TpMH_x$, which we hoped might be catalyst precursors for alkane conversions. We have recently reported[4] the first results of this work including the synthesis of $TpReH_6$, which is the first nitrogen-supported polyhydride. None of the Re complexes were catalytically active, and so we moved to Ir. As we will see below, we have not yet been able to prepare complexes of the $TpIrH_x$ type, but we were able to show that such systems would be very unlikely to act as alkane dehydrogenation catalysts. In the course of this work, we came upon a number of interesting and unexpected features of TpIr chemistry, which we report in this paper.

Results

In the hope of obtaining a labile system from which we could prepare the polyhydride, we attempted to make $TpIr(coe)_2$ (coe = cyclooctene) by the route shown in eq 1. In fact, the product turned out to be the cyclooctenyl hydride (**1**). The material is very soluble even in hexane and can be isolated as solvated powder.

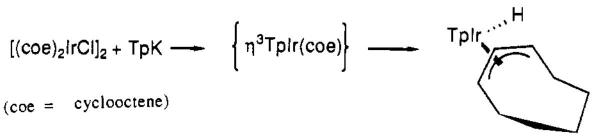

1

(1)

The proposed structure is consistent with the high-resolution mass spectrometric data and the ^1H and ^{13}C NMR spectra in toluene-d_8 at 25 °C. The ^1H NMR spectrum shows three sets of resonances for the Tp pyrazole rings, an Ir–H resonance at δ −18.1, and resonances corresponding to the vinylic CH protons of the coordinated cyclooctenyl group at 5.57 (t, 1 H), 4.54 (m, 1 H), and 4.04 ppm (m, 1 H). The J_{app} of 7.9 Hz is comparable to that observed by Faller and Chao[5] in a cyclooctenyl molybdenum complex. We do not observe any coupling between the Ir-H group and any allyl proton, in contrast to the situation in some other allyl hydrides.[6]

An η^3-Tp ligand has a high steric demand. As we shall see, only relatively unhindered olefins will give derivatives of the type (η^3-Tp)Ir(ol)$_2$. This suggests to us that one coe must dissociate before the three pyrazole rings can ligate to the Ir center in eq 1. The intermediate (η^3-Tp)Ir(coe) is related to the type "CpIrL" proposed by Bergman[7] and Graham and their co-workers for the photochemical activation of various C–H bonds. Here the same type of intermediate is formed, and an allylic C–H bond of the coordinated coe is activated to give **1**.

The symmetry of the complex is lower than expected; the three Tp pyrazole rings and the two ends of the allyl group are inequivalent (Figure 1). The molecule therefore lacks a plane of

---

(1) For a recent review of pyrazole-derived ligands and their complexes, see: Trofimenko, S. *Prog. Inorg. Chem.* **1986**, *34*, 115.

(2) Ghosh, C. K.; Graham, W. A. G. *J. Am. Chem. Soc.* **1987**, *109*, 4726. Hoyano, J. K.; Graham, W. A. G. *Abstracts of Papers*, 195th National Meeting of the American Chemical Society, Toronto, Canada; American Chemical Society: Washington, DC, 1988; INORG 216.

(3) (a) Burk, M. J.; Crabtree, R. H. *J. Am. Chem. Soc.* **1987**, *109*, 8025–8032. (b) Crabtree, R. H.; Parnell, C. P.; Uriarte, R. J. *Organometallics* **1987**, *6*, 696. (c) Crabtree, R. H.; Mihelcic, J. M.; Quirk, J. M. *J. Am. Chem. Soc.* **1982**, *104*, 107–113.

(4) Hamilton, D. G.; Luo, X.-L.; Crabtree, R. H. *Inorg. Chem.*, in press.

(5) Faller, J. W.; Chao, K.-H. *Organometallics* **1984**, *3*, 927.

(6) (a) McGhee, W. D.; Bergman, R. G. *J. Am. Chem. Soc.* **1988**, *110*, 4246–4262. (b) Cartura, G.; Scrivanti, A.; Morandini, F. *Angew. Chem., Int. Ed. Engl.* **1981**, *20*, 112. (c) Sherman, E. O.; Olson, M. *J. Organomet. Chem.* **1979**, *172*, C13.

(7) Janowicz, A. H.; Bergman, R. G. *J. Am. Chem. Soc.* **1982**, *104*, 352.

0020-1669/89/1328-3444$01.50/0 © 1989 American Chemical Society